Electronic Supplementary Material (ESI) for Nanoscale.

Supporting Information for

Binder-Free mechanochemical metal-organic framework nanocrystal coatings

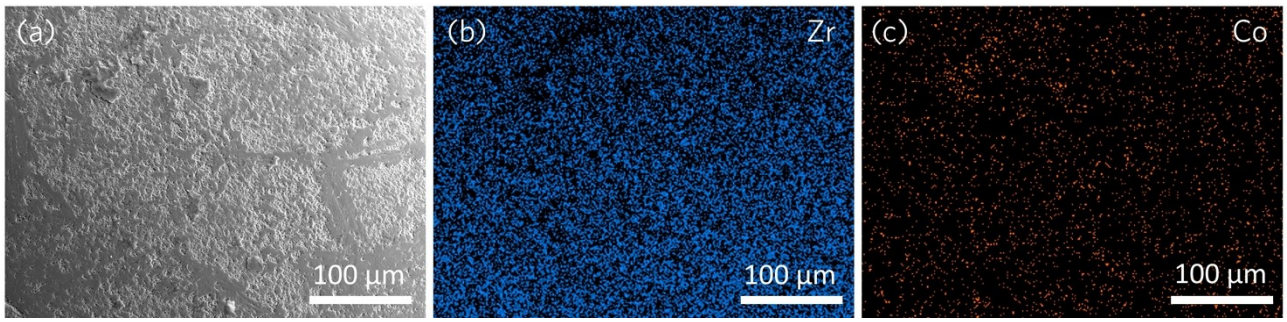

Fig. S1 (a) SEM image and (b, c) the corresponding EDS mapping of the used ZrO_2 ball surface.

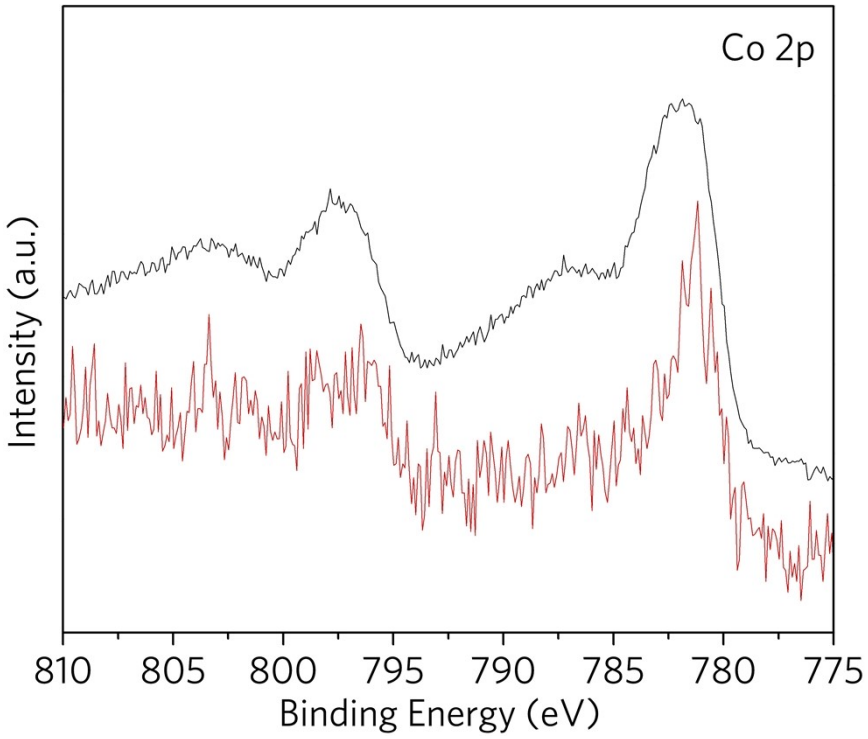

Fig. S2 XPS spectra (Co 2p) of Co-ZIF-62 (black) and used ZrO_2 ball after the Co-ZIF-62 synthesis (red).

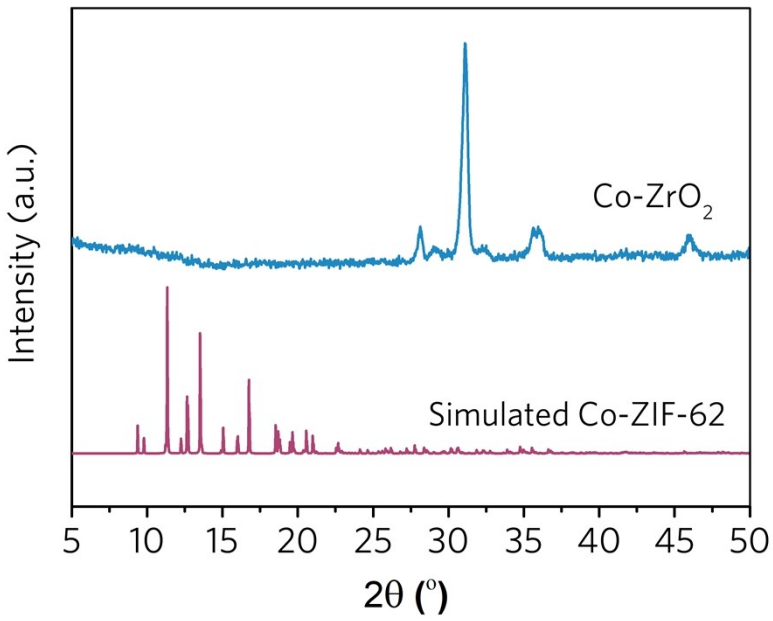

Fig. S3 XRD patterns of the simulated Co-ZIF-62 and the ZrO_2 balls after ball milling. These diffraction peaks are attributed to the ZrO_2.

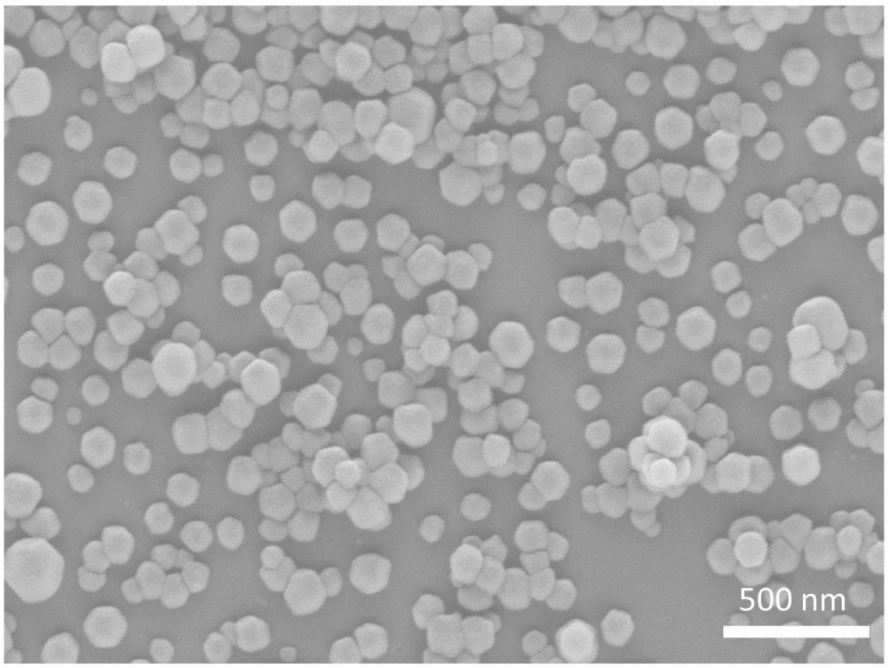

Fig. S4 SEM image of the presynthesised ZIF-8 crystals.

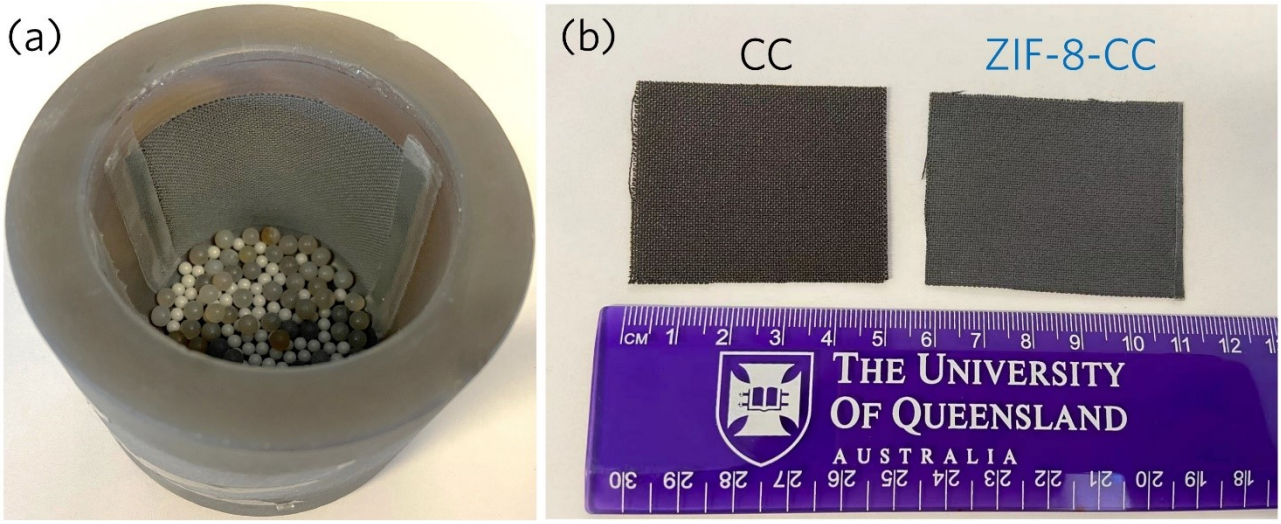

Fig. S5 (a) Optical photos of the mechanochemical coating process, and (b) carbon cloth (CC) before and after coated with ZIF-8.

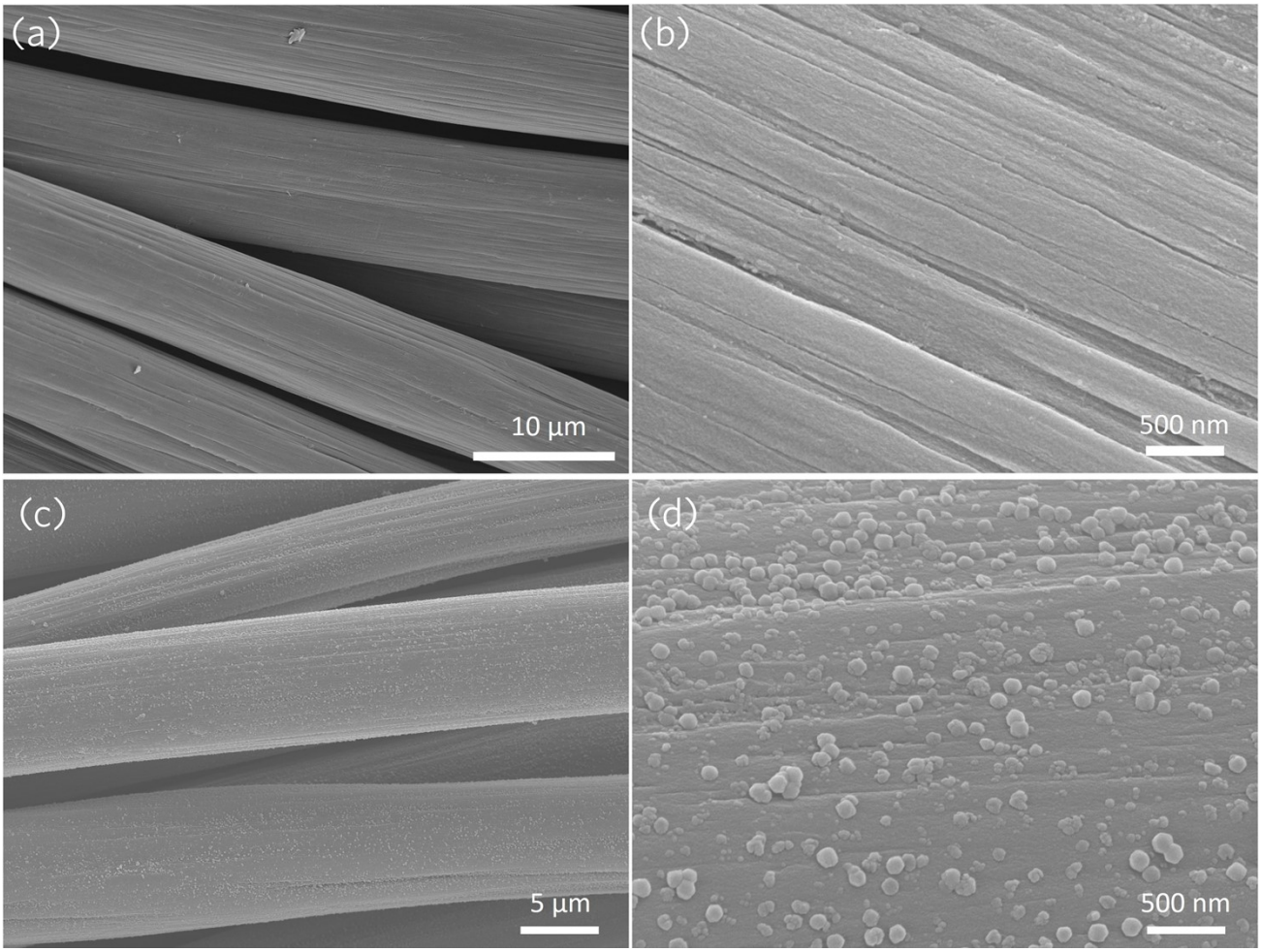

Fig. S6 SEM images of carbon cloth before (a, b) and after (c, d) coating with ZIF-8.

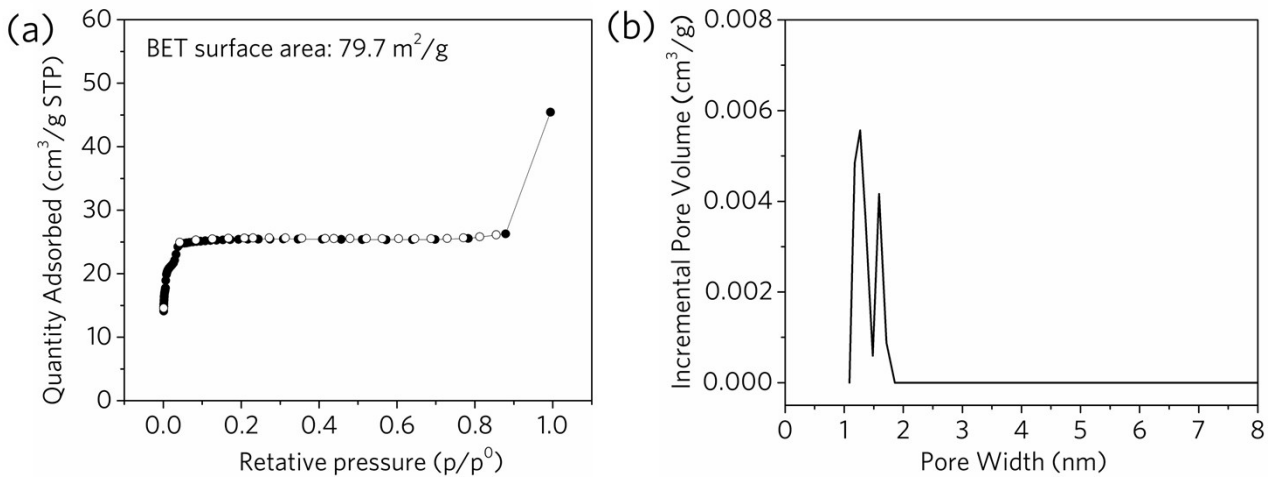

Fig. S7 (a) N_2 sorption isotherm at 77K (adsorption: closed symbols; desorption: open symbols) and (b) pore size distribution of ZIF-8-CC

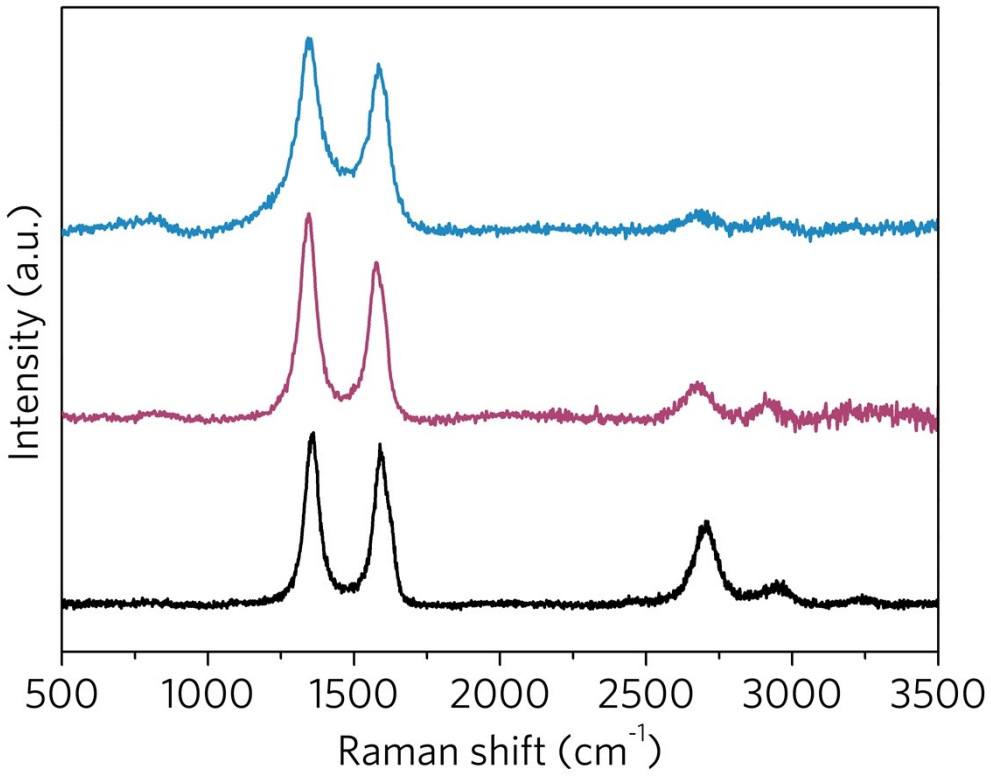

Fig. S8 Raman spectra of the carbon cloth after ball milling in different environments (bottom: before ball milling; middle: after ball milling in air; top: after ball milling in argon)

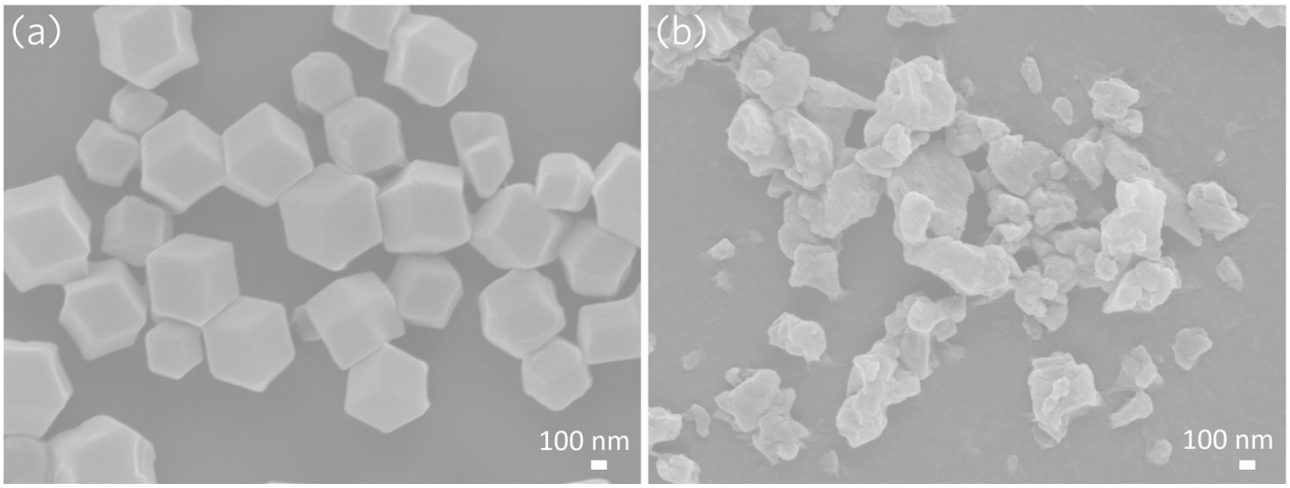

Fig. S9 SEM images of (a)ZIF-67 and (b) a_mZIF-67

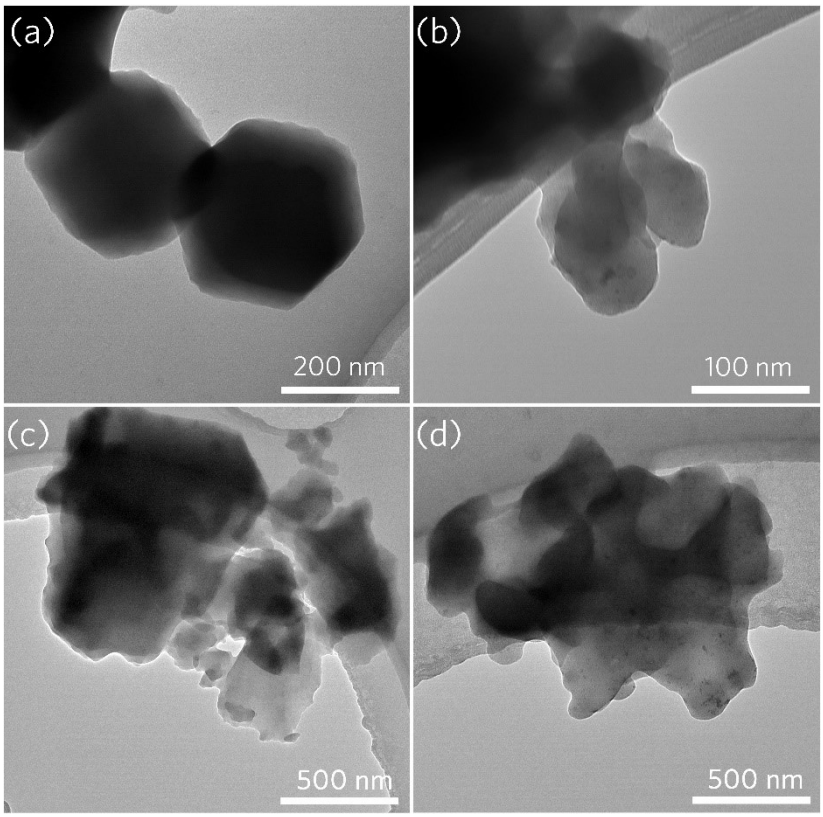

Fig. S10 TEM images of (a) ZIF-67, (b) a_mZIF-67, (c) Co-ZIF-4, and (d) a_gCo-ZIF-4

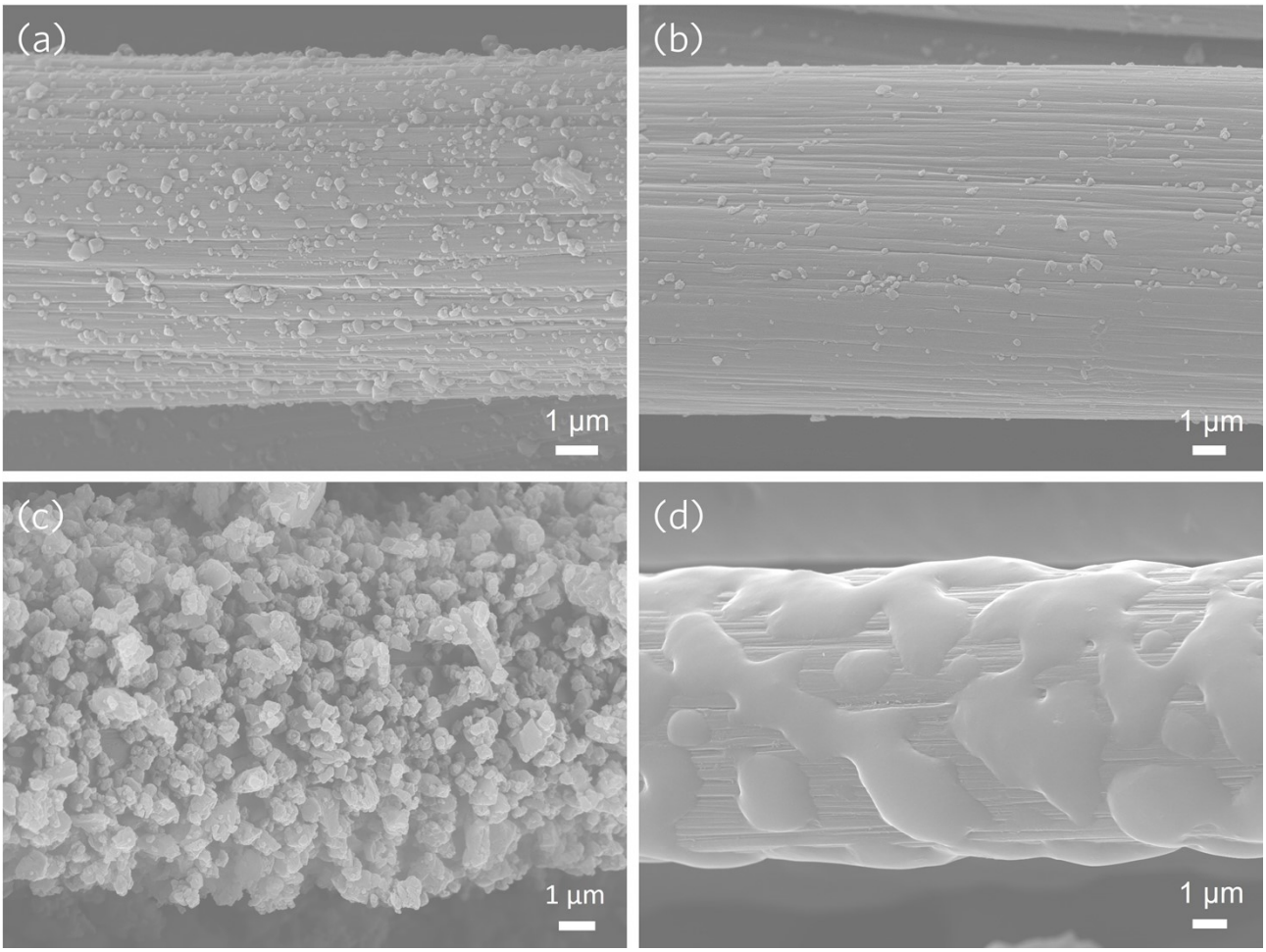

Fig. S11 SEM images (a) ZIF-67-CC, (b) a_mZIF-67-CC, (c) Co-ZIF-4-CC, and (d) a_gCo-ZIF-4-CC

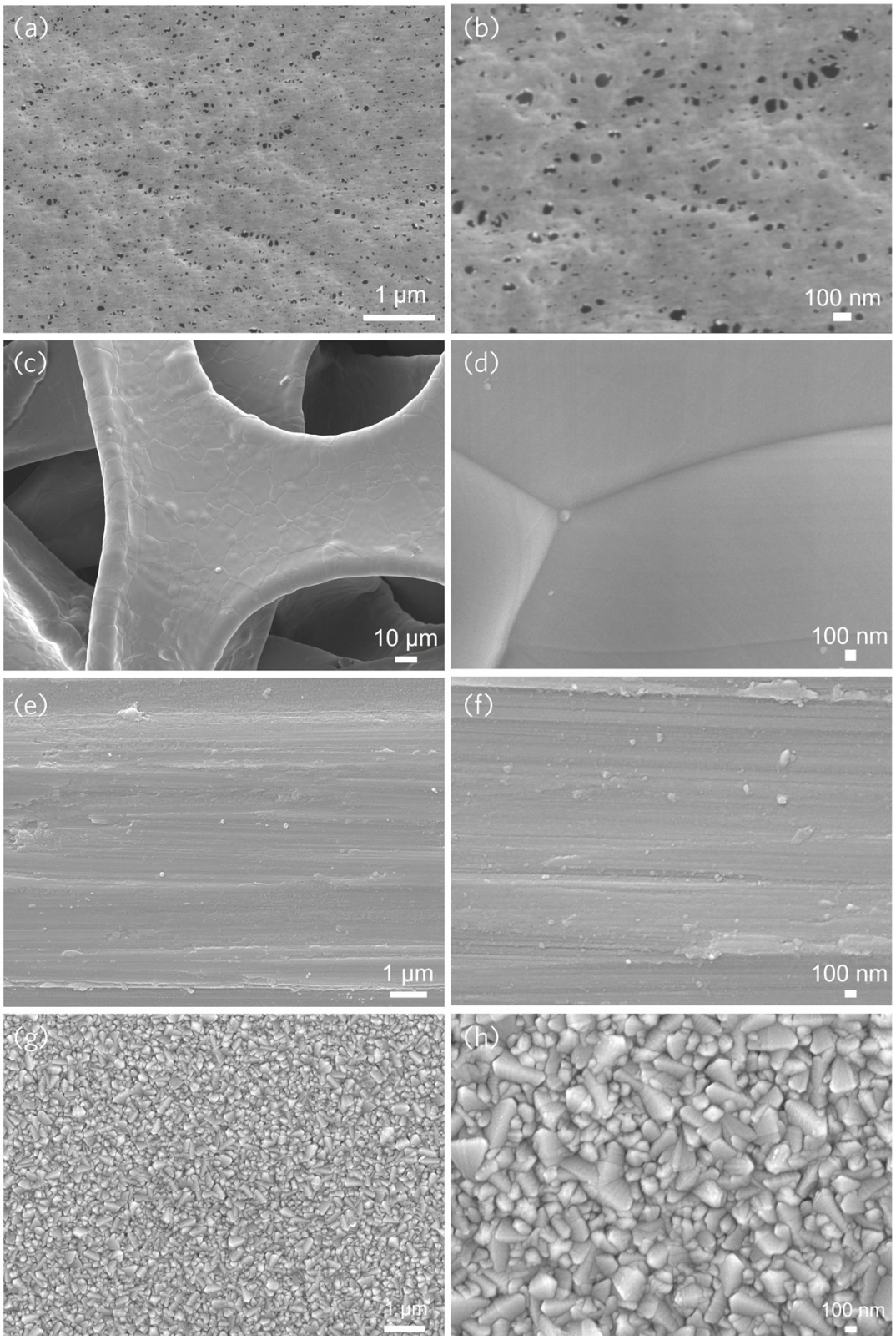

Fig. S12 SEM secondary electron images of substrates before coating procedure: (a, b) PVDF, (c, d) Ni foam, (e, f) Ti foil, (g, h) FTO.

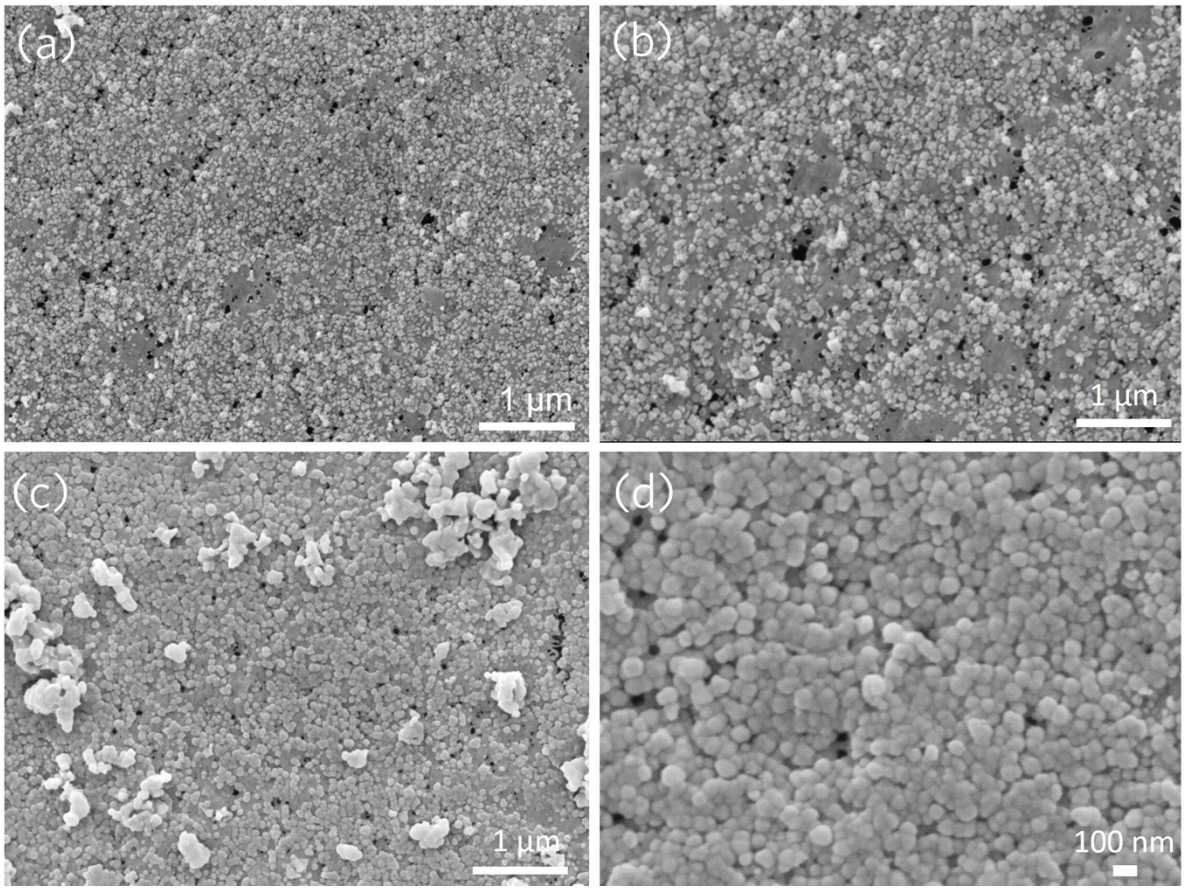

Fig. S13 ZIF-8 coating on PVDF *via* the one-pot technique. SEM images of ZIF-8 coating on PVDF prepared with (a, b) precursor: 0.005g ZnO and 0.01g 2-methylimidazole and (c, d) precursor: 0.01g ZnO and 0.02g 2-methylimidazole.

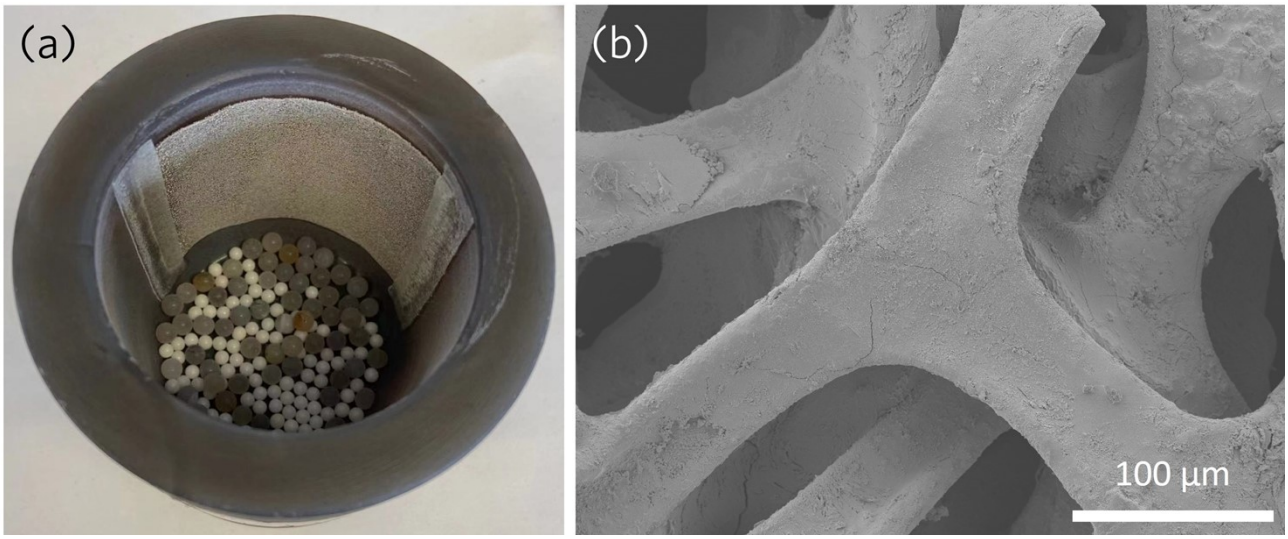

Fig. S14 (a) Optical photo and (b) SEM image of the ZIF-8 coating on the nickel foam.

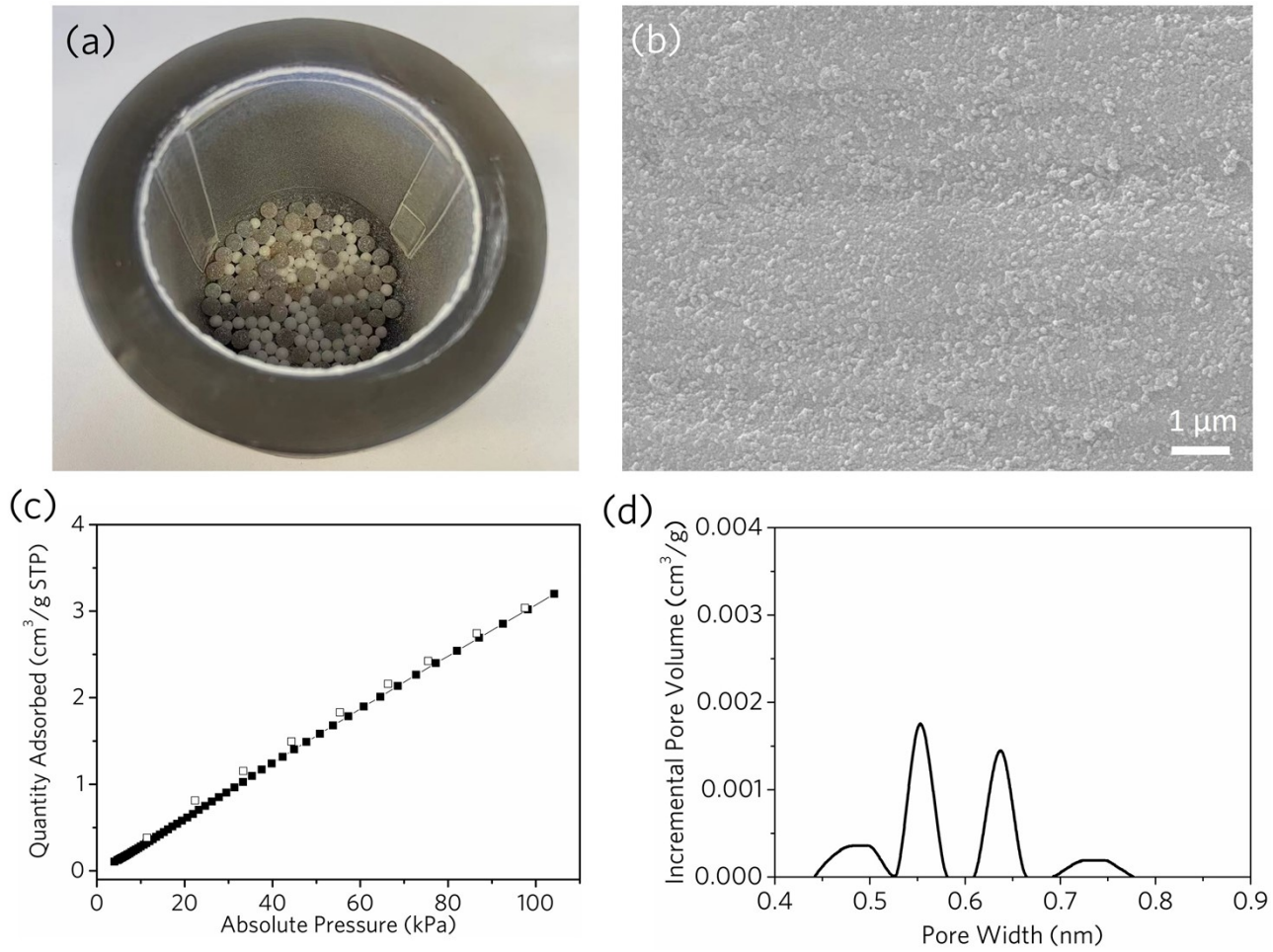

Fig. S15 (a) Optical photo and (b) SEM image of the ZIF-8 coating on a titanium foil. (c) CO_2 adsorption-desorption isotherms of ZIF-8-Ti at 273 K (adsorption: closed symbols; desorption: open symbols). (d) Pore size distribution of ZIF-8-Ti.

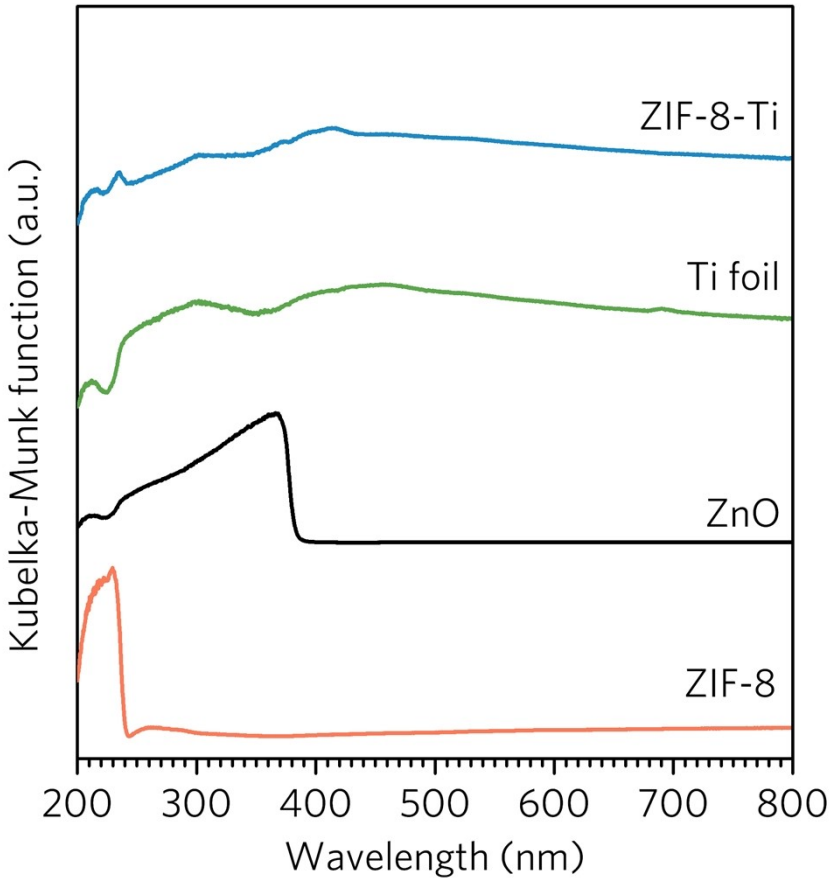

Fig. S16 Ultraviolet-visible (UV-Vis) absorption spectra for ZIF-8, ZnO, Ti foil and ZIF-8-Ti

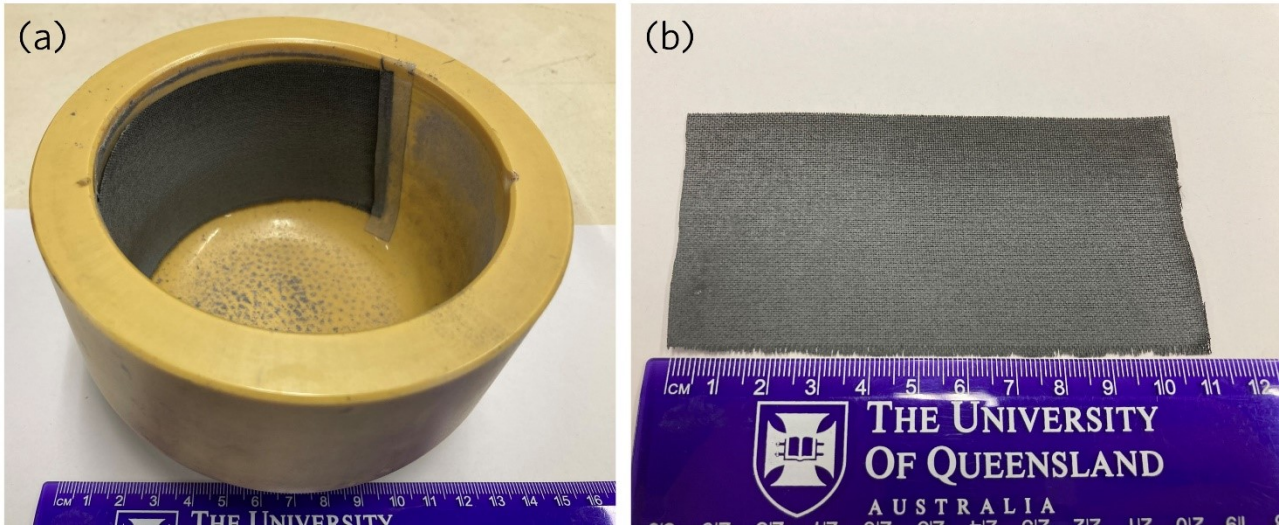

Fig. S17 Optical photos of the ZIF-8 coating on carbon cloth prepared by a large ball milling jar.

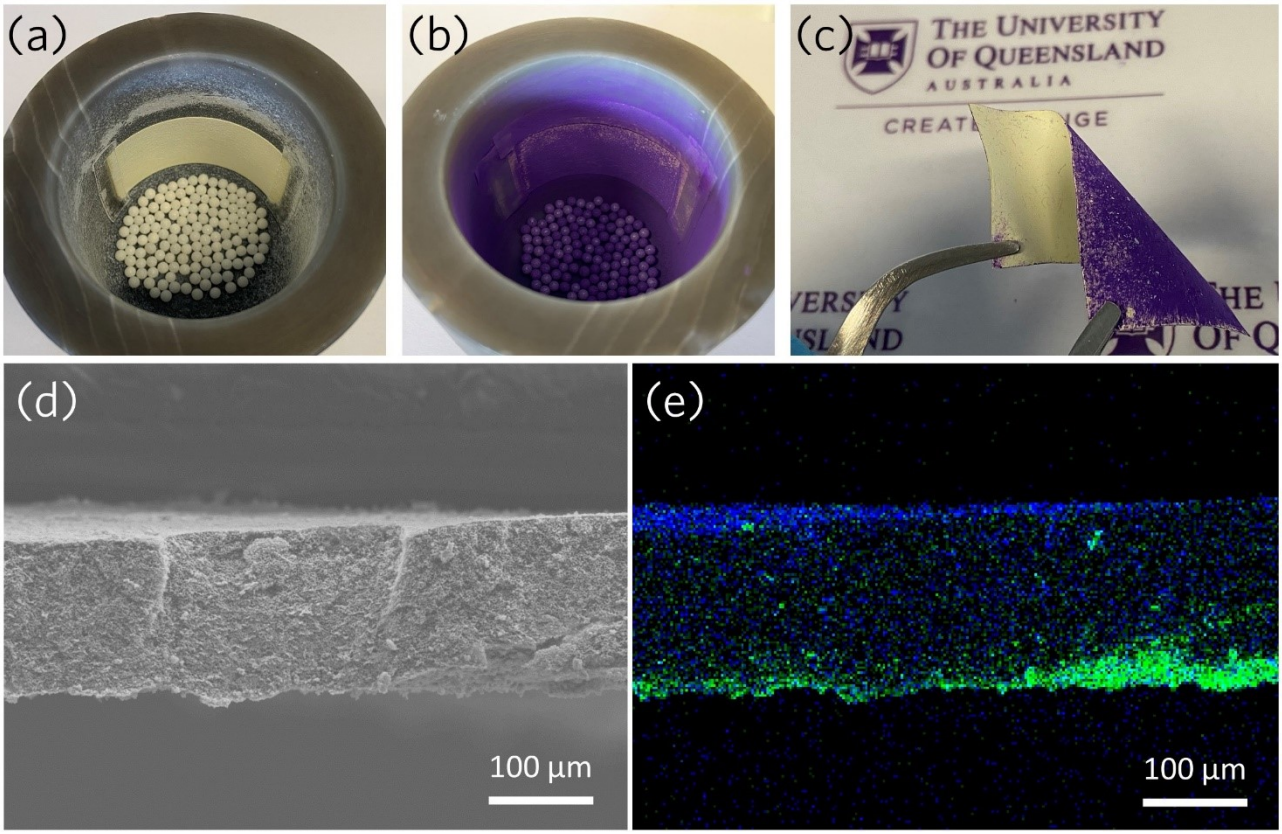

Fig. S18 (a-c) Optical photos of the dual side MOF coatings (ZIF-8 and Co-ZIF-62) on a porous Matrimid support. (d) SEM image and the cooresponding (e) EDS mapping of the cross-section of porous Matrimid with dual side MOF coating (Co in green and Zn in blue).

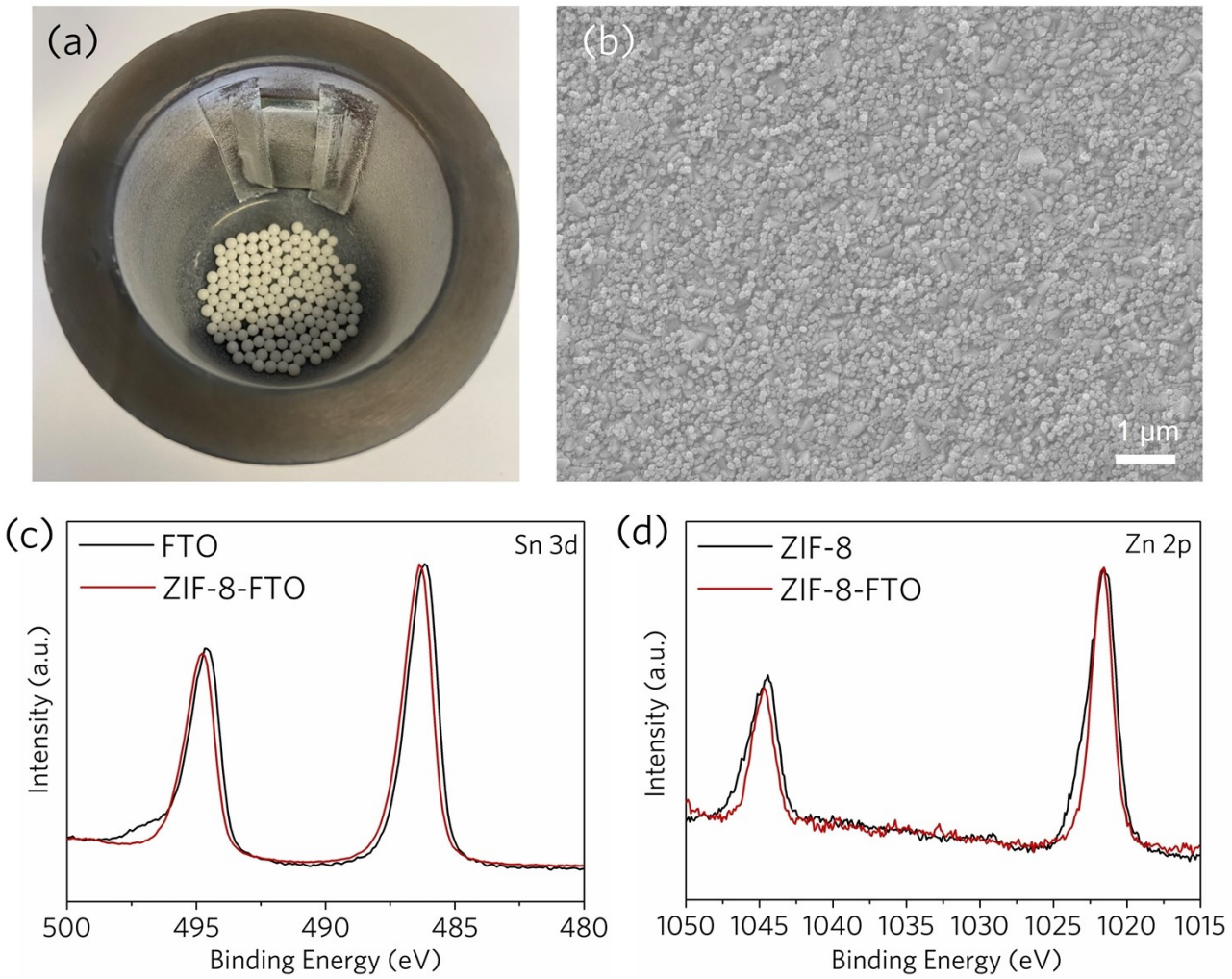

Fig. S19 (a) Photograph of the FTO taped on the inner wall of the ball milling jar. (b) SEM image of ZIF-8-FTO. (c-d) XPS spectra of ZIF-8-FTO (c: Sn 3d; d: Zn 2p).

Table S1 Loading of ZIF-8 on ZIF-8-CC samples before and after 100 cycles bending according to the ICP-OES results.

	Area (cm^2)	Total amount of Zn (mg)	Density of ZIF-8 on CC (mg cm^{-2})
ZIF-8-CC	4.0	1.48	1.31
ZIF-8-CC after 100 cycles bending	4.0	1.40	1.24

Table S2 Loading of MOFs on ZIF-67-CC, a_mZIF67-CC, Co-ZIF-4-CC and a_gCo-ZIF-4-CC according to the ICP-OES results.

	Area (cm^2)	Total amount of Co (mg)	Density of catalyst on CC (mg cm^{-2})
ZIF-67-CC as-synthesised	4.0	0.947	0.897
ZIF-67-CC after rinsing	4.0	0.035	0.032
a_mZIF67-CC as-synthesised	4.0	0.966	0.914
a_mZIF67-CC after rinsing	4.0	0.033	0.031
Co-ZIF-4-CC	4.0	1.472	1.218
a_gCo-ZIF-4-CC	4.0	1.476	1.222